J. Pharm. Pharmacol. 2000, 52: 1211–1221
Received April 18, 2000
Accepted June 9, 2000

The Effects of Carrier Size and Morphology on the Dispersion of Salbutamol Sulphate after Aerosolization at Different Flow Rates

XIAN MING ZENG*, GARY PETER MARTIN, CHRISTOPHER MARRIOTT AND JOHN PRITCHARD†

Department of Pharmacy, King's College London, Franklin-Wilkins Building, 150 Stamford Street, London SE1 8WA and †GlaxoWellcome Group Research Ltd, Park Road, Ware, Hertfordshire SG12 0DP, UK

Abstract

We have investigated the interdependence of various factors (particle size, surface smoothness, carrier particle shape, inhalation flow rate) on the deposition of a model drug (salbutamol sulphate) after aerosolization from a model inhaler device (Rotahaler).

Different batches of α-lactose monohydrate were prepared to have different particle size, particle shape and surface smoothness. Each batch of lactose was then mixed separately with salbutamol sulphate in a ratio of 67·5 : 1 (w/w), under similar conditions. Drug deposition from each formulation was investigated using a 4-stage liquid impinger after aerosolization at 28·3, 60·0 and 96·0 L min^{-1} via a Rotahaler.

At a flow rate of 28·3 L min^{-1}, a large portion of drug particles was not emitted from the inhaler, the % emission varying from 29·6% to 66·6% for all formulations investigated. Drug emission tended to increase with particle size of the carrier whilst fine particle fraction, fine particle dose and dispersibility appeared to increase with decreasing particle size but increasing elongation ratio of the carrier particles. Increasing the flow rate to 60 · 0 L min^{-1} was shown to increase drug emission since >75% total dose was found to be emitted from the inhaler. Again, smaller or more elongated lactose particles resulted in a higher fine particle dose or fine particle fraction of salbutamol sulphate than the coarser carrier, although they produced a similar (analysis of variance $P>0{\cdot}05$) drug emission. Increasing the flow rate to 96·0 L min^{-1} did not increase drug emission. Increasing the flow rate resulted in an increase in the fine particle fraction and fine particle dose of salbutamol sulphate from all formulations. The flow rate of the airstream appeared to play the most important role, followed by particle size and elongation ratio of the carrier particles, with the surface smoothness relatively less significant in determining the deposition of salbutamol sulphate from the Rotahaler.

In dry-powder formulations intended for inhalation, the micronized drug particles are either aggregated in a controlled manner to form loosely adherent floccules (e.g. Turbohaler) or are blended with coarser carrier particles (e.g. Rotahaler). α-Lactose monohydrate has been employed most frequently as the carrier and it is usually designed to have a size between 30–90 μm for this purpose (Timsina et al 1994). Depending on the specific requirement for the characteristics of the final blend such as flowability, other particle size distributions of lactose are also employed in the pharmaceutical industry. After blending with the carrier particles, the drug particles are usually present in low concentrations, determined by both the nominal dose and delivered mass of the powder per actuation, and the majority of the drug particles are thought to adhere to the carrier particles. On inhalation, the drug particles have to detach from the carrier and deaggregate into primary particles to gain access to the lower airways. Both the detachment and deaggreagation are a function of the energy input generated from the inhaled air stream and the physicochemical properties of the component particles such as surface texture (Ganderton 1992), particle size (French et al 1996; Steckel & Müller 1997) and particle shape (Zeng et al 2000a). The

*Present address: Inhalation Technology Department, Norton Healthcare Ltd, Albert Basin, Royal Docks, London E16 2QJ, UK.
Correspondence: G. P. Martin, Department of Pharmacy, King's College London, Franklin-Wilkins Building, 150 Stamford Street, London SE1 8WA, UK.
E-Mail: gary.martin@kcl.ac.uk

breath-actuation nature of dry-powder inhalers (DPIs) requires that sufficient energy be generated to detach the adhesive drug from its carrier and deaggregate any drug agglomerates. It is well documented that increasing inhalation flow rates generally increases the delivery efficiency of drugs from DPIs (Auty et al 1987; Hindle et al 1994). However, all those previous studies investigated these various factors separately, although in reality they act in an integrated manner to determine drug delivery by DPIs. Furthermore, the effect of a particular factor such as the carrier morphology on drug delivery would be expected to change with other factors such as inhalation flow rate. Therefore, we have investigated the interdependence of the various factors, including particle size, surface smoothness and particle shape of the carrier as well as the inhalation flow rate, on the deposition of a model drug, salbutamol sulphate, after aerosolization from a model inhaler device, the Rotahaler.

Materials and Methods

Materials

Salbutamol sulphate (volume median diameter 5·8 μm of geometric standard deviation 1·7), Ventolin Rotahaler and hard gelatin capsules (size 3) were supplied by GlaxoWellcome Research and Development Ltd (Ware, Hertfordshire, UK). α-Lactose monohydrate (Lactochem) was obtained from Borculo Whey Ltd (Chester, UK). *p*-Hydroxybenzoic acid ethyl ester was purchased from Sigma Chemical Co. (Poole, Dorset, UK), whilst ammonium acetate and methanol of HPLC grade were obtained from BDH Laboratory Supplies (Poole, Dorset, UK).

Preparation and characterization of lactose crystals

α-Lactose monohydrate was prepared by crystallization from aqueous solutions (Zeng et al 2000b). To prepare lactose crystals of different morphological features, the crystallization was carried out either by a two-stage crystallization without any additives, or by a one-step crystallization in the presence of a small amount (10%, v/v) of a water-miscible organic solvent such as ethanol and glycerine.

In the two-stage crystallization, the lactose solution (50% w/w) was first allowed to crystallize under constant stirring at room temperature at 500 rev min^{-1} for 2·5 h. The crystals (batch Aa′) were filtered and the mother liquor was placed back into the beaker and allowed to crystallize further for 16 h to obtain more crystals (batch Bb′). Both batches of crystals (Aa′ and Bb′) were washed with 60% (v/v) and absolute ethanol, respectively, and were allowed to dry at room temperature overnight. The crystals from batch Aa′ were fractionated by manual sieving to obtain particle sizes within the ranges of 63–90 μm (batch A) and <63 μm (batch a′). Batch Bb′ crystals were also fractionated into size fraction of 63–90 μm (batch B) and <63μm (batch b′). All crystals were then dried in a vacuum oven at 70°C for 3 h before transferring to a vial which was sealed and placed in a desiccator over silica gel, until required for further investigation.

In the one-step crystallization, a predetermined amount of an organic solvent (20 mL; ethanol or glycerine) was added dropwise to lactose solution (43%, w/w) such that the final concentration of the organic solvent in the solution was 10% (v/v). The crystallization was initiated by stirring the solution at room temperature at 500 rev min^{-1} until the majority of the crystals grew to a size between 63–90 μm. The crystals were filtered and washed with the 60% and absolute ethanol. Finally the crystals were allowed to dry at room temperature before being stored in a desiccator over silica gel. The harvested crystals were fractionated by manual sieving to obtain a particle size distribution between 63–90 μm. The crystals obtained in the presence of ethanol and glycerine were designated batches C and D, respectively.

A number of shape descriptors based on image analysis optical microscopy and surface area measurement were used to quantify the shape of lactose crystals. In the image analysis, a small amount of lactose particles was scattered on a microscope slide using a small brush ensuring that the particles deposited separately. The slide was then mounted on an optical microscope (Labophot-2, Nikon, Japan) and the images of the particles were transferred to an IBM compatible computer through a Nikon camera. Particle images were analysed automatically using analySIS 2.0 software (SIS Image Analysis GmbH, Germany). The size of each individual particle was calculated as the diameter of a spherical particle that produceds a projected image of the same area to the measured particle. At least 300 particles were measured for each batch of lactose and the surface-volume mean diameter (d_{sv}) recorded. The morphology of lactose crystals was quantified by three shape descriptors, derived from the length (L), width (W), perimeter (P) and area (A) of the projected image of a particle. These include the elongation ratio (E : L/W), the shape factor (F_{shape}: $4\pi \times A/P^2$) and the surface factor ($F_{surface}$: $F_{shape} \times (1+E)^2/(\pi \times E)$)

(Zeng et al 2000a). The higher the value of E the more elongated the particle. F_{shape} is also in the range 0–1 and combines properties relating to both surface roughness and shape (e.g. a spherical particle with a smooth surface has a value of 1). $F_{surface}$ is a derived factor, which also varies from 0–1 but is primarily dependent upon surface roughness alone; particles that are perfectly smooth would have a value of 1 (Zeng et al 2000a). The specific surface area of the powder was measured by air permeation using Fisher subsieve sizing apparatus (Zeng et al 2000b).

There were no two equivalent batches of lactose in terms of these shape descriptors (Table 1) and this was supported by the visual comparison of their scanning electron micrcrographs (Figure 1), which showed that different batches of lactose had different surface textures and shapes.

Blending lactose with salbutamol sulphate

Salbutamol sulphate was mixed separately with different batches of lactose in a ratio of 1 : 67·5 (w/w), in accordance with the ratio employed in the commercial Ventolin formulation. Salbutamol sulphate was weighed into a 10-mL stoppered sample vial to which had been added one spatula full of lactose crystals. The vial was stoppered and placed on a Whirlymixer for 5 s. More lactose particles (similar to the amount of the blend) were then added to the vial and the blend was mixed on a Whirlymixer for another 5 s. This process was repeated until all the lactose (1·750 g) had been incorporated into the salbutamol sulphate/lactose blend to obtain a ratio of drug to carrier of 1 : 67·5 (w/w). The stoppered vials were placed in a Turbula mixer (Glen Creston Ltd, Middlesex, UK) and mixed for 30 min. The samples were then stored in a vacuum desiccator over silica gel until further required.

Hard gelatin capsules (size 3) were filled with 33·0 ± 1·5 mg of the powder mixture so that each capsule contained 481 ± 22 μg salbutamol sulphate, which was the unit dose contained in a Ventolin Rotacap. The filling was performed manually.

HPLC analysis of salbutamol sulphate

Salbutamol sulphate was analysed by HPLC. The mobile phase was a mixture of methanol and 0·1% w/w aqueous ammonium acetate (45 : 55, pH 4·5) running at a flow rate of 0·8 mL min^{-1}, *p*-hydroxybenzoic acid ethyl ester (2 μg mL^{-1}) was the internal standard and UV detection was at 276 nm. The HPLC system consisted of a pump (CM 4000 Multiple Solvent Delivery System, LDC Analytical Inc., FL), a multiple wavelength UV detector (SpectroMonitor 3100, LDC Analytical Inc., FL) and a 15 cm × 4·6 mm i.d. column packed with 5 μm C-18 (Hypersil, Phenomenex, Cheshire, UK).

Deposition test

A sample of the HPLC mobile phase (20 mL) with internal standard was introduced to each of the upper stages of a 4-stage liquid impinger. A Whatman filter paper (<0.45 μm) was placed in stage 4 of the impinger. The throat was connected to the neck of the upper stage and wrapped with Sellotape to ensure the connection was airtight. A Rotahaler (GlaxoWellcome Group Ltd, Ware, Hertfordshire, UK) was then fitted into the moulded rubber mouthpiece attached to the throat of the impinger. Finally, a capsule was mounted in the inhaler device. Once the assembly had been checked and found to be airtight and the inhaler device, when inserted, was aligned with the horizontal axis of the throat of the impinger, the vacuum pump was switched on. The pump was run for 5 s to establish the flow rate of the airstream and then the dose was released. Following the release of the dose the pump was allowed to run for 7 s at 60 ± 1 L min^{-1} and was then switched off. The capsule shells were removed from the inhaler

Table 1. The surface–volume diameter (d_{sv}), specific surface area (S_a) and shape descriptors of different batches of crystallized lactose.

Batch no.	d_{sv} (μm) (n>300)	S_a (cm^2 g^{-1})	Shape factor (n>150)	Elongation ratio (n>150)	Surface factor (n>150)
A	104·7 ± 15·8	921·7	0·65 ± 0·08	1·79 ± 0·31	0·90 ± 0·09
a′	68·6 ± 15·8	1400·6	0·65 ± 0·10	1·55 ± 0·30	0·87 ± 0·11
B	96·0 ± 18·6	865·8	0·69 ± 0·12	1·81 ± 0·45	0·96 ± 0·14
b′	65·3 ± 18·7	1233·6	0·72 ± 0·11	1·54 ± 0·33	0·96 ± 0·13
C	93·7 ± 15·1	770·8	0·76 ± 0·12	1·25 ± 0·19	0·98 ± 0·14
D	103·7 ± 12·3	709·2	0·74 ± 0·12	1·82 ± 0·27	1·03 ± 0·14

Values are mean ± s.d. Batch A, lactose crystallized at the first stage (63–90 μm). Batch a′, lactose crystallized at the first stage (<63 μm). Batch B, lactose crystallized at the second stage (63–90 μm). Batch b′, lactose crystallized at the second stage (<63 μm). Batch C, lactose crystallized in the presence of ethanol. Batch D, lactose crystallized in the presence of glycerine.

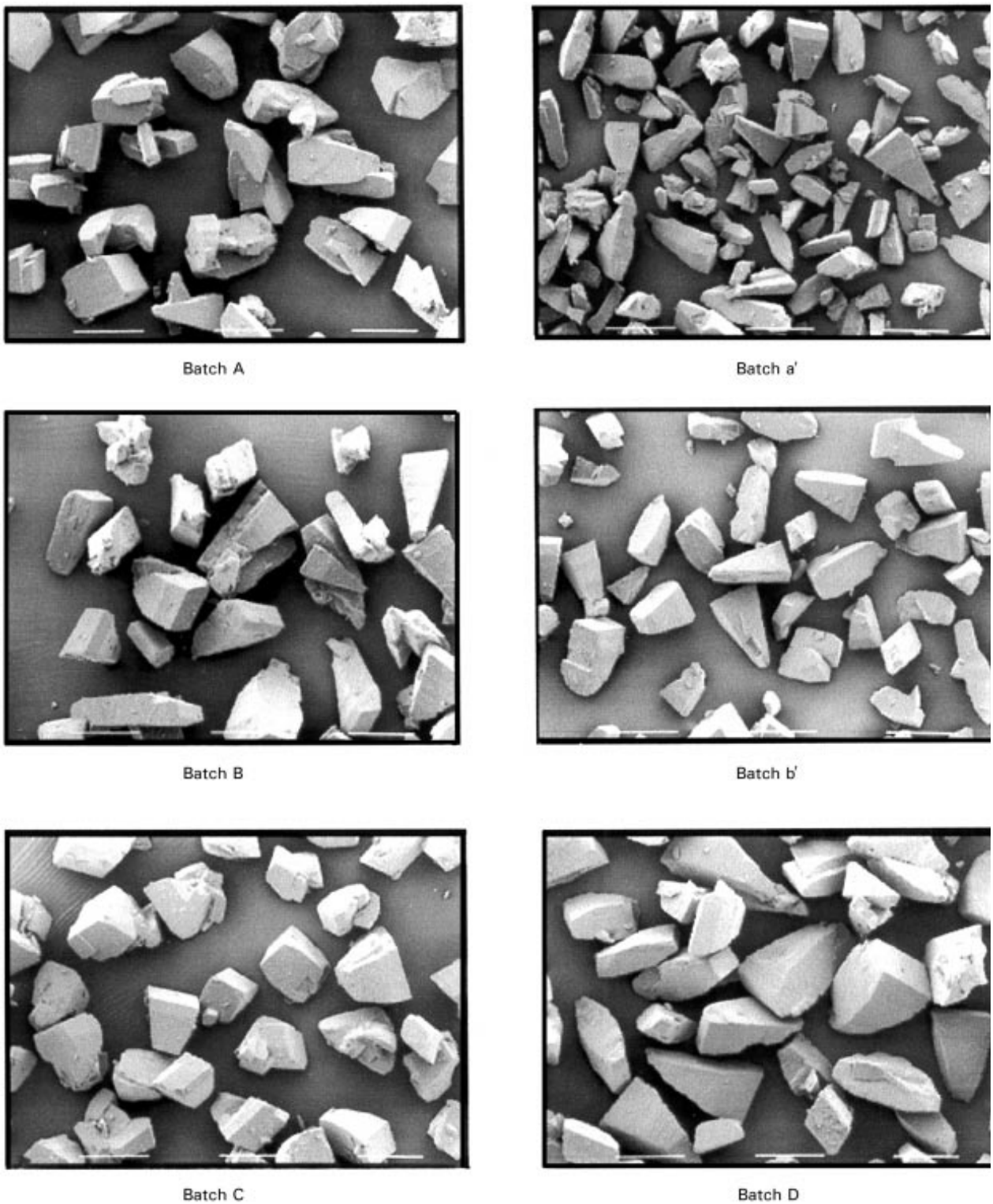

Figure 1. Scanning electron micrographs of different batches of lactose. Batch A, lactose crystallized at the first stage (63–90 μm). Batch a′, lactose crystallized at the first stage (<63 μm). Batch B, lactose crystallized at the second stage (63–90 μm). Batch b′, lactose crystallized at the second stage (<63 μm). Batch C, lactose crystallized in the presence of ethanol. Batch D, lactose crystallized in the presence of glycerine. Scale bars represent 100 μm.

device and the deposition test was repeated until four more capsules were actuated in the same manner.

Stage 4 of the impinger was then dismantled and the filter paper was carefully transferred to a beaker. The filter was washed three times with the mobile phase containing internal standard and the washing solution was transferred to a 50-mL volumetric flask and made up to volume with the same solvent. The inhaler body, capsule shells and mouthpiece were washed five times with the mobile phase and the washing solution was made up to 100 mL with the same solvent. The throat was washed three times with approximately 25 mL mobile phase and transferred to a 100-mL volumetric flask. The inside of the inlet jet tube to stage 1 was rinsed with the solvent and the washing solution was allowed to flow back into the stage. After transferring the solution to the same volumetric flask containing the washing solution from the throat, stage 1 was washed with the same solvent for three times and the final washing solution of this stage and the throat was made up to volume with the solvent. The solution in stage 2 was transferred to a 50-mL volumetric flask and the inside of the stage was washed three times with the mobile phase before making up to volume with the same solvent. Stage 3 was washed using the same procedure as that for stage 2. The concentration of salbutamol sulphate of all the samples obtained was analysed using the HPLC method as outlined above.

Similar deposition tests were carried out at flow rates of 28·3 and 96 L min^{-1} following the same operational and washing procedures. Each experiment was carried out four times.

Data analysis

A variety of parameters were employed to characterize the deposition profiles of salbutamol sulphate in the multistage liquid impinger. The recovered dose was the sum of the drug collected in the inhaler device, throat piece and four stages of the impinger, whilst the emitted dose was the amount of drug released from the inhaler device. The effective cut-off diameter of the impinger changes with airflow rate (Hugosson et al 1993). The fine particle dose was the amount of drug collected in stage 4 for aerosolization at 28·3 L min^{-1} (<4·5 μm). However, the fine particle dose was taken as the sum of the amounts in stages 3 and 4 for aerosolization at either 60·0 (<6·8 μm) or 96·0 L min^{-1} (<5·4 μm). The fine particle fraction was calculated as the ratio of fine particle dose to recovered dose whilst the dispersibility is the ratio of fine particle dose to emitted dose. The total recovery (% recovery) of the drug was assessed by the ratio of the recovered dose to the theoretical dose, the latter being the dose of salbutamol sulphate in the capsules. The % emission was calculated as the ratio of the emitted dose to the total dose.

Results and Discussion

Deposition at 28·3 L min^{-1}

After actuation at 28·3 L min^{-1} via a Rotahaler, the recovered dose of salbutamol sulphate per capsule varied from 414 μg for blends containing batch A lactose to 439 μg for blends composed of batch a′ lactose, corresponding to a % recovery of 86·1–91·3% (Table 2). The average recovery of all seven formulations was 89·2%. A large portion of drug particles were not emitted from the inhaler with an average emission of 50%, indicating that a flow rate of 28·3 L min^{-1} was not able to efficiently deliver the drug-lactose blends from a Rotahaler. Drug emission tended to depend on the particle size of lactose, a larger size fraction (63–90 μm) of the carrier particles producing higher emission of the drug than the smaller size fraction (<63 μm). For example, batch A lactose with a mean diameter of

Table 2. The deposition profiles of salbutamol sulphate in a 4-stage liquid impinger after aerosolization at 28·3 L min^{-1} via a Rotahaler.

Batch no.	Recovered dose (μg)	Emitted dose (μg)	Fine particle dose (μg)	Fine particle fraction (%)	Dispersibility (%)	Recovery (%)	Emission (%)
A	414 (2)	169 (24)	11 (3)	2·6 (0·8)	6·5 (2·4)	86·1 (1·7)	40·8 (2·8)
a′	439 (20)	130 (22)	25 (2)	5·7 (0·8)	19·3 (4·7)	91·3 (2·1)	29·6 (5·9)
B	431 (8)	287 (7)	15 (1)	3·5 (0·3)	5·2 (0·5)	89·6 (1·4)	66·6 (5·7)
b′	436 (10)	166 (30)	27 (1)	6·2 (0·2)	16·2 (2·5)	90·6 (4·1)	38·1 (4·1)
C	433 (15)	274 (9)	6 (0)	1·3 (0·0)	2·1 (0·1)	90·0 (3·2)	63·3 (1·1)
D	421 (3)	255 (13)	16 (1)	3·9 (0·3)	6·4 (0·8)	87·5 (0·6)	60·5 (2·9)

Values are mean (s.d.), n = 4. Batch descriptions as for Table 1.

104·7 μm (Table 1) was fractionated from the same batch of lactose crystals as batch a′, which had a mean diameter of 68·6 μm. The blends containing batch A lactose produced a significantly higher ($P<0{\cdot}01$) emission of the drug than those containing batch a′ lactose (Table 2). Similarly, a higher drug emission ($P<0{\cdot}05$) occurred from formulations containing batch B lactose (d_{sv}, 96·0 μm) than from formulations produced using batch b′ lactose (d_{sv}, 65·3 μm). It was also likely that the higher emission observed for blends containing either batch C or D lactose was primarily due to the lactose having a mean diameter >90 μm.

More powders were found to adhere to the inner walls of the inhaler device after actuation of the blends composed of finer lactose than those containing coarser lactose, leading to a lower percentage of drug emission from the former than from the latter blends. Once the powders were released from the capsules, either the freely dispersed drug particles or the carrier particles (with adhered drug particles) may be entrained in the air stream. The air-borne particles are likely to impact on the inner walls of the inhaler due to the turbulent airflow within the device, which is an essential design feature, introduced to aid particle dispersion and entrainment (Timsina et al 1994). Under specific aerosolization conditions, the detachment of any deposited particles from the device walls is akin to the detachment of particles from a stationary surface, which is dependent upon the particle size of the adherent particles. For example, the airflow velocity, required to dislodge 50% of adhered particles from a stationary surface, was shown to be inversely proportional to the particle size, regardless of the surface characteristics (Gotoh et al 1994). Therefore, smaller particles are more difficult to dislodge from their adhered sites than larger particles and hence, once impacted upon the wall of the inhaler device, smaller carrier particles with adhered drug particles are less likely to become airborne than larger particles. This might explain why the blends of smaller carrier particles produced lower drug emission from the inhaler device than the blends containing larger carrier particles. However, neither the blends of the smaller lactose particles nor those of the larger lactose particles produced efficient drug emission at 28·3 L min^{-1}, indicating that such a flow rate is insufficient to extract drugs from the Rotahaler.

The blends composed of finer lactose particles (batch a′ and b′) produced a fine particle dose almost twice as high as those of the blends containing their corresponding coarser lactose particles (batch A and B), although the former produced lower drug emission than the latter blends. Accordingly, the blends containing finer lactose particles produced significantly ($P<0{\cdot}01$) higher drug fine particle fraction than the blends of coarser lactose particles. The finer lactose produced a dispersibility of salbutamol sulphate three times as high as that of the corresponding coarser lactose particles. These results strongly suggest that

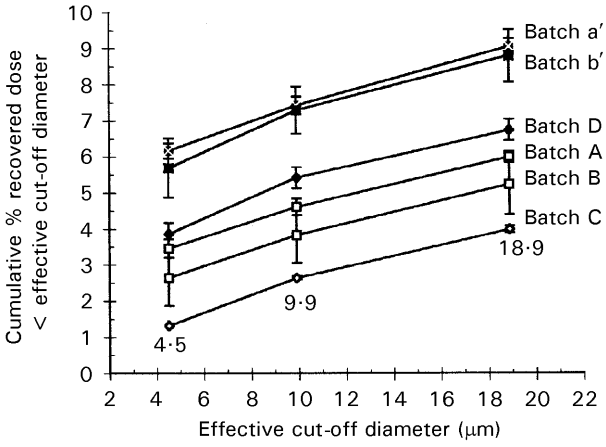

Figure 2. The particle size distribution of salbutamol sulphate after aerosolization from different batches of lactose at 28·3 L min^{-1} via a Rotahaler. Batch A, lactose crystallized at the first stage (63–90 μm). Batch a′, lactose crystallized at the first stage (<63 μm). Batch B, lactose crystallized at the second stage (63–90 μm). Batch b′, lactose crystallized at the second stage (<63 μm). Batch C, lactose crystallized in the presence of ethanol. Batch D, lactose crystallized in the presence of glycerine. Error bars denote standard deviation, n = 4.

Table 3. Details of regression and analysis of variance of the relationship between drug fine particle fraction and carrier morphology at 28·3 L min^{-1}.

Predicator	Fine particle fraction (% recovered dose)			Dispersibility		
	SEQ SS	t-ratio	*P*	SEQ SS	t-ratio	*P*
Diameter (μm)	24·9	−7·40	0·000	552·7	−7·98	0·000
Elongation ratio	16·5	5·31	0·000	85·7	3·16	0·007
Surface factor	6·2	−1·09	0·292	0·0	0·06	0·950

SEQ SS = sequential sum of squares.

adhered drug particles were more likely to detach from finer carrier than from coarser carrier.

From the particle size, elongation ratio and surface factor of different batches of lactose, it might be possible to establish the relationship between drug fine particle fraction and morphology of lactose. Thus, the following empirical equations (1 and 2) were generated by 'step-wise forward algorithm' in multiple regression using a Minitab for Windows (Version 10.2).

$$\text{Fine particle fraction} = 4{\cdot}92E - 4{\cdot}26F_{surface} - 0{\cdot}0968d + 8{\cdot}54 \quad r^2 = 0{\cdot}853 \tag{1}$$

$$\text{Dispersibility} = 11{\cdot}7E + 1{\cdot}0F_{surface} - 0{\cdot}418\,d + 26{\cdot}1 \quad r^2 = 0{\cdot}846 \tag{2}$$

where d, E and $F_{surface}$ are the mean diameter (μm), elongation ratio and 'surface factor' of lactose particles, respectively. The statistical details of the regression analysis are shown in Table 3.

Thus, the fine particle fraction and dispersibility of salbutamol sulphate decreased with the mean diameter of lactose particles ($P<0{\cdot}01$), confirming that smaller carrier particles produced higher fine particle fraction of the drug. Increasing the elongation ratio of the carrier particles increased the fine particle fraction and dispersibility of the drug ($P<0{\cdot}01$), in agreement with previous results achieved using a twin impinger operated at a flow rate of 60 L min^{-1} (Zeng et al 2000a). However, the surface smoothness, expressed by the value of 'surface factor', did not show any significant effect ($P>0{\cdot}05$) on the fine particle fraction and dispersibility of salbutamol sulphate.

The blends containing lactose batches a′ and b′ produced aerosolized salbutamol sulphate of similar particle size and size distribution. The particle size distribution of the deposited drug was similar for blends containing lactose A and B, although the plots of cumulative % recovered dose as a function of effective cut-off diameter were less than those obtained for batches a′ and b′ (Figure 2). The highest % recovered dose of drug particles with aerodynamic diameter (d_a) <18·9 μm observed for the blends containing lactose batch a′ or b′ indicated that the finer carrier produced more efficient aerosolization of drug than the coarser carrier.

Deposition at 60·0 L min^{-1}

After aerosolization at 60·0 L min^{-1} via a Rotahaler, the average drug recovery of all the deposition tests was 94·7% (Table 4). All the blends had a similar percentage of drug emission with an average of 78·9% recovered dose from the inhaler device, indicating that a flow rate of 60·0 L min^{-1} was able to dislodge the aerosol blends from the inhaler device. Hindle et al (1994)

Table 4. The deposition profiles of salbutamol sulphate in a 4-stage liquid impinger after aerosolization at 60·0 L min^{-1} via a Rotahaler.

Batch no.	Recovered dose (μg)	Emitted dose (μg)	Fine particle dose (μg)	Fine particle fraction (%)	Dispersibility (%)	Recovery (%)	Emission (%)
A	442(18)	362(10)	76(6)	14·7(1·3)	18·1(2·6)	94·5(2·9)	81·2(3·9)
a′	448(24)	348(20)	90(3)	17·5(1·3)	23·3(1·2)	94·0(2·9)	74·9(3·5)
B	455(14)	370(29)	67(4)	17·1(1·0)	20·9(1·2)	91·7(3·6)	81·9(1·9)
b′	453(14)	339(27)	79(8)	20·0(0·5)	25·8(0·7)	92·9(4·9)	77·6(1·6)
C	474(10)	384(26)	52(4)	10·9(1·0)	13·5(1·8)	98·5(2·0)	80·9(3·8)
D	464(3)	356(5)	71(2)	15·2(0·3)	19·8(0·4)	96·3(0·6)	76·7(0·7)

Values are mean (s.d.), n = 4. Batch descriptions as for Table 1.

Table 5. Details of regression and analysis of variance concerning the relationship between drug fine particle fraction and morphology of carrier particles at 60·0 L min^{-1}.

Predicator	Fine particle fraction (% recovered dose)			Dispersibility		
	SEQ SS	t-ratio	*P*	SEQ SS	t-ratio	*P*
Diameter (μm)	62·8	−10·02	0·000	134·2	−10·54	0·000
Elongation ratio	73·2	8·35	0·000	131·8	7·62	0·000
Surface factor	2·7	1·58	0·137	4·2	1·52	0·151

SEQ SS = sequential sum of squares.

reported that increasing the flow rate of an inhaled air stream increased the emission of drug from inhaler devices. Smaller lactose carrier particles (batch a′ or b′) still produced slightly lower drug emission than their corresponding larger lactose (batch A or B). However, unlike aerosolization at 28·3 L min^{-1}, the dependence of drug emission on carrier particle size became statistically insignificant ($P>0.05$) at an aerosolization flow rate of 60·0 L min^{-1}.

Similar to the deposition at 28·3 L min^{-1}, lactose crystals of smaller size fraction produced higher fine particle dose or fine particle fraction of salbutamol sulphate. For example, the fine particle dose and fine particle fraction of salbutamol sulphate from batch a′ lactose was significantly higher ($P<0.05$) than the corresponding values using batch A lactose. These results further confirm that the formulations containing smaller carrier particles produced more efficient delivery of the drug from DPIs than those containing carriers of a larger particle size.

To evaluate the relationship between drug fine particle fraction and particle morphology of lactose, the following empirical equations (3 and 4) were generated by 'step-wise forward algorithm' in multiple regression using a Minitab for Windows (Version 10.2).

$$\text{Fine particle fraction (\% recovered dose)} = 11{\cdot}2E + 8{\cdot}9F_{surface} - 0{\cdot}19d + 6{\cdot}0 \quad r^2 = 0{\cdot}901 \tag{3}$$

$$\text{Dispersibility} = 13{\cdot}3E + 11{\cdot}1F_{surface} - 0{\cdot}259d + 11{\cdot}1 \quad r^2 = 0{\cdot}904 \tag{4}$$

where d, E and $F_{surface}$ are as defined as before. The statistical details of the regression analysis are shown in Table 5.

Thus, drug fine particle fraction and dispersibility was again shown to be inversely proportional to the mean diameter of lactose carrier particles ($P<0.01$). Increasing carrier elongation ratio also increased the fine particle fraction and dispersibility of the drug ($P<0.01$). An increase in the surface smoothness, expressed by the value of the 'surface factor', only resulted in a slight but insignificant increase in both parameters ($P>0.05$). Thus, similar to the deposition at a flow rate of 28·3 L min^{-1}, particle size and shape (elongation) of the lactose particles played a more important role in determining the fine particle fraction of salbutamol sulphate than surface smoothness.

The inclusion of lactose particles derived from batch b′ in the drug formulation resulted in the most efficient aerosolization of salbutamol sulphate, with the highest fraction of aerosolized salbutamol sulphate with $d_a<13{\cdot}0\ \mu m$ (Figure 3). Batches a′ and B

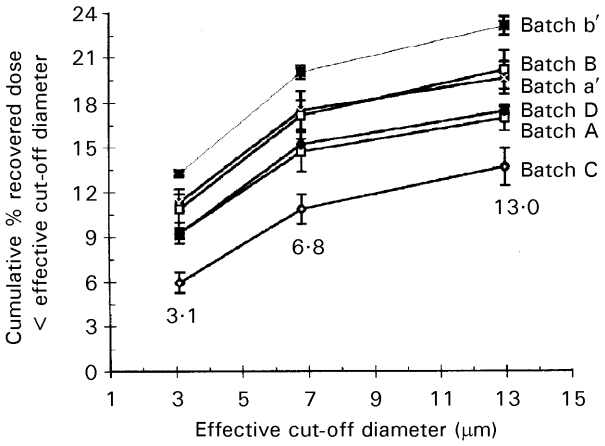

Figure 3. The particle size distribution of salbutamol sulphate after aerosolization using different batches of lactose at 60·0 L min^{-1} via a Rotahaler. Batch A, lactose crystallized at the first stage (63–90 μm). Batch a′, lactose crystallized at the first stage (<63 μm). Batch B, lactose crystallized at the second stage (63–90 μm). Batch b′, lactose crystallized at the second stage (<63 μm). Batch C, lactose crystallized in the presence of ethanol. Batch D, lactose crystallized in the presence of glycerine. Error bars denote standard deviation, n = 4.

Table 6. The deposition profiles of salbutamol sulphate in a 4-stage liquid impinger aerosolization at 96·0 L min^{-1} via a Rotahaler.

Batch no.	Recovered dose (μg)	Emitted dose (μg)	Fine particle dose (μg)	Fine particle fraction (%)	Dispersibility (%)	Recovery (%)	Emission (%)
A	444(5)	337(9)	104(9)	19·2(0·6)	24·6(1·8)	95·7(0·6)	78·3(3·3)
a′	455(17)	353(14)	118(9)	24·3(0·9)	31·5(1·1)	98·6(0·4)	77·1(0·6)
B	461(3)	361(15)	89(3)	23·4(1·7)	30·9(2·0)	92·2(1·0)	75·9(1·2)
b′	475(2)	366(4)	115(5)	25·8(1·9)	33·3(1·8)	94·4(3·6)	77·7(1·5)
C	473(13)	389(11)	59(4)	12·4(0·6)	15·0(0·7)	98·2(2·7)	82·2(0·5)
D	458(16)	343(14)	101(1)	21·9(0·7)	29·3(1·1)	95·1(3·3)	74·8(1·0)

Values are mean (s.d.), n = 4. Batch descriptions as for Table 1.

Table 7. Details of regression and analysis of variance concerning the relationship between drug fine particle fraction and lactose morphology at an aerosolization flow rate of 96·0 L min^{-1}.

Predicator	Fine particle fraction (% recovered dose)			Dispersibility		
	SEQ SS	t-ratio	*P*	SEQ SS	t-ratio	*P*
Diameter (μm)	102·7	−13·53	0·000	160·8	−13·84	0·000
Elongation ratio	245·7	14·03	0·000	498·0	15·28	0·000
Surface factor	5·8	2·13	0·049	15·7	2·67	0·018

SEQ SS = sequential sum of squares.

produced a similar pattern of drug aerosolization. Formulations containing either batch A or batch D lactose produced a similar particle size distribution of salbutamol sulphate in the impinger, which was lower than the comparable distributions resulting from formulations containing batch a′ or batch B lactose (Figure 3). Lactose batch C resulted in the lowest amount of drug particles being aerosolized. The highest fraction of aerosolized drug particles with d_a<13·0 μm, which resulted from blends containing lactose batch b′ may be attributable to the smaller particle size and smooth surface of this batch of carrier particles. Although batch a′ lactose had a smaller mean diameter (68·6 μm) than batch B (96·0 μm), the former crystals had a more irregular shape with a rougher surface than the latter crystals. The two opposing factors counteract each other, leading to a more or less similar aerosolization of salbutamol sulphate from these batches of lactose. Batch A lactose had a mean diameter of 104·7 μm and the particles possessed a rough surface (Table 1). This batch of lactose produced fewer aerosolized drug particles compared with batches a′, B or b′. Batch C had a less elongated shape than batch D lactose. This may be the major factor that resulted in the lowest fine particle fraction being produced from formulations containing batch C lactose.

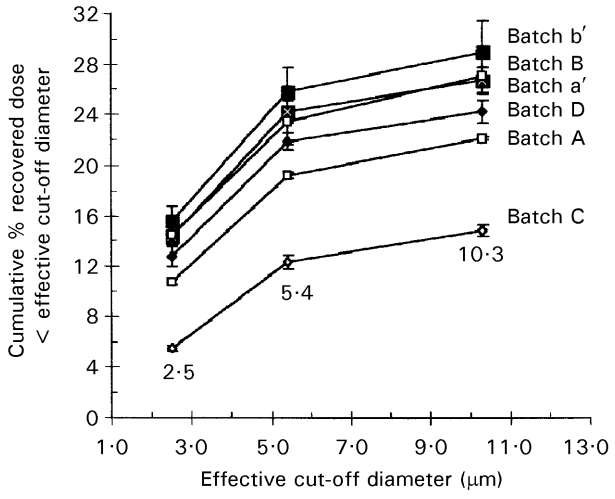

Figure 4. The particle size distribution of salbutamol sulphate after aerosolization from different batches of lactose at 96·0 L min^{-1} via a Rotahaler. Batch A, lactose crystallized at the first stage (63–90 μm). Batch a′, lactose crystallized at the first stage (<63 μm). Batch B, lactose crystallized at the second stage (63–90 μm). Batch b′, lactose crystallized at the second stage (<63 μm). Batch C, lactose crystallized in the presence of ethanol. Batch D, lactose crystallized in the presence of glycerine. Error bars denote standard deviation, n = 4.

Deposition at 96·0 L min^{-1}

After aerosolization at 96·0 L min^{-1} via a Rotahaler, the average drug recovery was 95·7% (Table 6), which was slightly but insignificantly (P>0·05) higher than the average recovery measured at 60·0 L min^{-1}. All the blends showed a drug recovery over 90% nominal dose, which was indicative of an accurate, reproducible experimental procedure encompassing mixing and capsule filling, through deposition, to drug analysis. Similar drug emission was found for all blends, with an average emitted dose of 77·7% recovered dose being obtained. There was no significant difference in the drug emission after aerosolization at 60·0 and 96·0 L min^{-1}, indicating that increasing the flow rate did not result in a corresponding increase in the emission of the drug from a Rotahaler.

To evaluate the relationship between the drug fine particle fraction and carrier particle morphology, the following empirical equations (equations 5 and 6) were generated by 'step-wise forward algorithm' in multiple regression using a Minitab for Windows (Version 10.2).

$$\text{Fine particle fraction} = 20{\cdot}4E + 13{\cdot}0F_{surface} - 0{\cdot}278d + 0{\cdot}16 \quad r^2 = 0{\cdot}952 \tag{5}$$

$$\text{Dispersibility} = 29{\cdot}2E + 21{\cdot}4F_{surface} - 0{\cdot}373d - 7{\cdot}38 \quad r^2 = 0{\cdot}956 \tag{6}$$

Details of the statistical analysis are listed in Table 7.

Similar to the results achieved at flow rates of 28·3 and 60·0 L min^{-1}, the drug fine particle fraction and

dispersibility were found to increase with decreasing particle size of lactose ($P<0{\cdot}01$). In addition, the more elongated the carrier particles the higher the fine particle fraction of the drug ($P<0{\cdot}01$). The surface smoothness of the carrier appeared to exert a significant effect on the fine particle fraction ($P<0{\cdot}05$) at this flow rate, drug fine particle fraction increasing with the surface smoothness of the carrier particles. However, the effect of elongation ratio of lactose carrier particles appeared to be more pronounced than that of the particle size since the former factor produced a higher absolute value of the t-ratio than the latter factor (Table 7). These results suggest that whilst the effects of elongation ratio and surface smoothness of lactose particles on drug deposition may become more prominent at $96{\cdot}0\,\mathrm{L\,min^{-1}}$, the effect of particle size might diminish at this flow rate.

The differences in the particle size distribution of salbutamol sulphate from different batches of lactose was less pronounced after an aerosolization flow rate of $96{\cdot}0\,\mathrm{L\,min^{-1}}$ (Figure 4) as compared with that observed after aerosolization at flow rates of either 28·3 or $60{\cdot}0\,\mathrm{L\,min^{-1}}$. However, lactose batch a′ still produced a significantly more efficient ($P<0{\cdot}01$) aerosolization of the drug than batch A lactose, although the use of batch b′ lactose appeared to result in a similar pattern of drug aerosolization to batch B. Furthermore, the cumulative % recovered dose of salbutamol sulphate using batch D lactose was more than twice that found after use of batch C lactose.

Analysis of the deposition data obtained at different aerosolization flow rates

The fine particle fraction and dispersibility of salbutamol sulphate from different batches of lactose particles obtained at different aerosolization flow rates were analysed by 'step-wise forward algorithm' in multiple regression using a Minitab for Windows (Version 10.2). The following empirical equations (equations 7 and 8) were generated so as to evaluate the effects of aerosolization flow rates and particle morphology of lactose carrier particles on the deposition of salbutamol sulphate.

$$\text{Fine particle fraction} = 0{\cdot}253\mathrm{V} + 12{\cdot}0\mathrm{E} + 5{\cdot}6\mathrm{F_{surface}} - 0{\cdot}188\mathrm{d} - 10{\cdot}2 \qquad r^2 = 0{\cdot}905 \tag{7}$$

$$\text{Dispersibility} = 0{\cdot}267\mathrm{V} + 18{\cdot}0\mathrm{E} + 11{\cdot}2\mathrm{F_{surface}} - 0{\cdot}35\mathrm{d} - 6{\cdot}45 \qquad r^2 = 0{\cdot}904 \tag{8}$$

where V is the aerosolization flow rate ($\mathrm{L\,min^{-1}}$); d, E, $\mathrm{F_{surface}}$ are as defined previously. Details of the statistical analysis are listed in Table 8.

Thus, aerosolization flow rate plays the most important role (the highest value of either SEQ salbutamol sulphate or t-ratio) in determining the fine particle fraction of salbutamol sulphate, an increase in the flow rate resulting in an increase in the fine particle fraction of the drug. The aerosolization flow rate is critical in determining both the dispersion and deaggregation of entrained particle agglomerates.

Increasing particle size of the lactose carrier decreased the fine particle fraction of salbutamol sulphate. Thus, in terms of drug detachment from air-borne carrier particles, smaller carrier particles may appear to be more favourable than larger carrier particles. However, smaller particles have poorer flowability than larger particles, which may result in other problems during powder handling processes. An optimized particle size of the carrier should therefore ensure maximum drug delivery without sacrificing other powder properties such as flowability. This can be achieved by the modification of particle morphology of lactose carrier.

The elongation ratio of lactose particles appears to be of a similar importance in affecting the fine particle fraction of salbutamol sulphate to particle size. Increasing the elongation ratio of the carrier particles resulted in an increase in the fine particle

Table 8. The details of regression and analysis of variance of the relationship between drug fine particle fraction and aerosolization flow rates as well as particle morphology of lactose.

Predicator	Fine particle fraction (% recovered dose)			Dispersibility		
	SEQ salbutamol sulphate	t-ratio	*P*	SEQ salbutamol sulphate	t-ratio	*P*
Flow rate	2654·2	20·05	0·000	2945·2	17·79	0·000
Diameter (μm)	179·4	−6·95	0·000	760·8	−10·93	0·000
Elongation ratio	258·7	6·27	0·000	578·6	7·96	0·000
Surface factor	3·2	0·70	0·489	12·8	1·17	0·247

fraction of the drug regardless of the aerosolization flow rates and inhaler devices. Although increasing the surface smoothness of the carrier particles resulted in a slight increase in the fine particle fraction of the drug, this effect was not of statistical significance ($P>0{\cdot}05$). However, it must be remembered that the definition of fine particle fraction changed with flow rates. Fine particle fractions obtained at different flow rates covered different size fractions of the aerosolized drug, the fine particle fraction at 28·3, 60 and 96 L min^{-1} being defined as particles $<4{\cdot}5$, 6·8 and 5·4 μm, respectively. Therefore, the combined analysis of the fine particle fraction obtained at different flow rates only provides a semi-quantitative insight into the effects of different factors on the deposition of the drug.

Conclusion

Inhalation flow rate played the most important role in determining the dispersion and deaggregation of salbutamol sulphate from the Rotahaler. Although all DPIs are breath-actuated, the dependence of drug-delivery efficiency on inhalation flow rate should ideally be kept minimal so as to minimize any variation in therapeutic effects due to the variable patients' inspiratory effort. Reducing the relationship between inhalation flow rate and drug delivery has been one of the major goals in developing novel dry-powder inhalers. The particle size and particle shape of the carrier crystals appeared to exert opposing effects, to a similar extent, on drug dispersion and deaggregation. If large carrier particles are required to be incorporated into a formulation, it is still possible to achieve relatively high delivery efficiency of the drug by means of engineering the carrier particles to have a precisely defined shape.

Acknowledgements

This study was financially supported by an Overseas Research Studentship and a GlaxoWellcome Studentship for X. M. Zeng. During the writing of this paper, X. M. Zeng was a Maplethorpe Fellow.

References

Auty, R. M., Brown, K., Neale, M. G., Snashall, P. D. (1987) Respiratory tract deposition of sodium cromoglycate is highly dependent upon technique of inhalation using the Spinhaler. Br. J. Dis. Chest 88: 371–378

French, L., Edwards, D. A., Niven, R. W. (1996) The influence of formulation on emission, deaggregation and deposition of dry powders for inhalation. J. Aerosol Sci. 27: 769–783

Ganderton, D. (1992) The generation of respirable clouds from coarse powder aggregates. J. Biopharm. Sci. 3: 101–105

Gotoh, K., Kida, M., Masuda, H. (1994) Effect of particle diameter on removal of surface particles using high speed air jet. Kagaku Kogaku Ronbunshu 20: 693–700

Hindle, M., Jashnani, R. N., Byron, P. R. (1994) Dose emissions from marketed inhalers: influence of flow, volume and environment. In: Byron, P., Farr, S. (eds) Respiratory Drug Delivery IV. CRC Press, Boca Raton, Florida pp 137–142

Hugosson, S., Lindberg, J., Loof, T., Olsson, B. (1993) Proposals for standardized testing of powder preparations for inhalation. Pharm. Form. 19: S458–S466

Steckel, H., Müller, B. W. (1997) In vitro evaluation of dry powder inhalers II: influence of carrier particle size and concentration on in vitro deposition. Int. J. Pharm. 154: 31–37

Timsina, M. P., Martin, G. P., Marriott, C., Ganderton, D., Yianneskis, M. (1994) Drug delivery to the respiratory tract using dry powder inhalers. Int. J. Pharm. 101: 1–13

Zeng, X. M., Martin, G. P., Marriott, C., Pritchard, J. (2000a) The influence of carrier morphology on drug delivery by dry powder inhalers. Int. J. Pharm. 200: 93–106

Zeng, X. M., Martin, G. P., Marriott, C., Pritchard, J. (2000b) The influence of crystallization conditions on the morphology of lactose intended for use as a carrier for dry powder aerosols. J. Pharm. Pharmacol. 52: 633–643